Human B lymphoblastoid cells contain distinct patterns of cathepsin activity in endocytic compartments and regulate MHC class II transport in a cathepsin S-independent manner

Alfred Lautwein,[*,†] Marianne Kraus,[*,†] Michael Reich,[*,†] Timo Burster,[*,†] J. Brandenburg,[†] Herman S. Overkleeft,[‡] Gerold Schwarz,[§] Winfried Kammer,[§] Ekkehard Weber,[¶] Hubert Kalbacher,[†] Alfred Nordheim,[§] and Christoph Driessen[*,†,1]

Department of Medicine II, [†]Medical and Natural Sciences Research Centre, and [§]Institute for Cell Biology, Department Molecular Biology, University of Tübingen, Germany; [‡]Leiden Institute of Chemistry, Gorleaus Laboratory, The Netherlands; and [¶]Institute of Physiological Chemistry, University of Halle, Germany

Abstract: Endocytic proteolysis represents a major functional component of the major histocompatibility complex class II antigen-presentation machinery. Although transport and assembly of class II molecules in the endocytic compartment are well characterized, we lack information about the pattern of endocytic protease activity along this pathway. Here, we used chemical tools that visualize endocytic proteases in an activity-dependent manner in combination with subcellular fractionation to dissect the subcellular distribution of the major cathepsins (Cat) CatS, CatB, CatH, CatD, CatC, and CatZ as well as the asparagine-specific endoprotease (AEP) in human B-lymphoblastoid cells (BLC). Endocytic proteases were distributed in two distinct patterns: CatB and CatZ were most prominent in early and late endosomes but absent from lysosomes, and CatH, CatS, CatD, CatC, and AEP distributed between late endosomes and lysosomes, suggesting that CatB and CatZ might be involved in the initial proteolytic attack on a given antigen. The entire spectrum of protease activity colocalized with human leukocyte antigen-DM and the C-terminal and N-terminal processing of invariant chain (Ii) in late endosomes. CatS was active in all endocytic compartments. Surprisingly and in contrast with results from dendritic cells, inhibition of CatS activity by leucine–homophenylalanine–vinylsulfone-phenol prevented N-terminal processing of Ii but did not alter the subcellular trafficking or surface delivery of class II complexes, as deferred from pulse-chase analysis in combination with subcellular fractionation and biotinylation of cell-surface protein. Thus, BLC contain distinct activity patterns of proteases in endocytic compartments and regulate the intracellular transport and surface-delivery of class II in a CatS-independent manner. *J. Leukoc. Biol.* 75: 844–855; 2004.

Key Words: *antigen presentation · endocytic proteases*

INTRODUCTION

Antigen presentation by major histocompatibility complex (MHC) class II molecules relies on the coordinated interaction of class II complexes and their associated molecules [human leukocyte antigen (HLA)-DM, HLA-DO] with trafficking and proteolysis along the endocytic route. The class II-associated invariant chain (Ii) and antigenic protein must undergo proteolytic processing during their endocytic transport before class II peptide loading and presentation of immunogenic epitopes to antigen-specific T cells can occur. As limited proteolysis rather than total breakdown is the rule in both proteolytic pathways, a well-balanced proteolytic environment is required to ensure proper class II function [1, 2].

In contrast to the cytosolic MHC class I-associated processing pathway dominated by the proteasome, class II-associated endocytic compartments of antigen-presenting cells (APC) contain a multitude of active proteolytic enzymes that can participate in proteolytic destruction. The major portion of these proteases belongs to the cathepsin (Cat) family, whose members mostly share the structural and functional properties of papain-like cysteine proteases (CatS, CatL, CatB, CatH, CatZ, CatC), although noncathepsin endocytic proteases such as the asparagine-specific endopeptidase (AEP) are likely to be equally important [3, 4]. In contrast to AEP, which exclusively cleaves after asparagine residues, cysteine–cathepsins lack narrowly defined substrate specificities but show partially overlapping cleavage preferences within hydrophobic regions of a given protein [5, 6]. In spite of this low-substrate specificity, which implicates a high degree of functional redundancy, individual cathepsins are essential in mediating discrete, proteolytic steps during breakdown of Ii and exogenous protein in intact APC in a nonredundant manner [7–11]. Thus, to mediate limited proteolysis, proteolytic activity is likely to be guided by

[1] Correspondence: MNF Universität Tübingen, Ob dem Himmelreich 7, 72074 Tübingen, Germany. E-mail: christoph.driessen@med.uni-tuebingen.de

Received August 6, 2003; revised December 21, 2003; accepted January 12, 2004; doi: 10.1189/jlb.0803367.

cellular mechanisms other than the mere substrate specificity of the proteases present in the endocytic tract.

Individual endocytic proteases differ in their pH optima as well as their affinity for endogenous protease inhibitors and are subject to transport along the endocytic pathway. As local pH and redox conditions gradually change during the transit from early endosomes to late endosomes and lysosomes, individual activity patterns of endocytic proteases might be present at different endocytic locations and activation stages, which in turn, could represent a key element in regulating class II function [12]. Such differential content and activity of endocytic proteases have been demonstrated for the phagosome of murine macrophages, which gradually acquires different endocytic enzymes during its maturation [13]. In these cells, exogenous material ingested by phagocytosis encountered CatZ and CatB early after incorporation into the phagosome, and only further maturation of the phagosome exposed the internalized material to the remaining papain cathepsins.

Highly specialized, late endosomal/prelysosomal compartments for class II processing and peptide loading, termed MHC class II-associated compartment (MIIC; refs. [14–18]), characterize the endocytic machinery of human B cells. The analysis of Ii processing in human B-lymphoblastoid cells (BLC) has led to major insights into the function of endocytic proteases as well as the architecture of this endocytic compartment. Degradation of Ii is initiated by C-terminal processing in a late endosomal/prelysosomal compartment [16, 18, 19]. It involves cysteine proteases, an aspartate protease, and AEP activity, leading ultimately to the generation of Iip10, a fragment that consists of the class II-binding portion of Ii [termed class II Ii-associated peptide (CLIP)] attached to the intact N terminus of Ii, including the transmembrane domain and the cytoplasmic-sorting signal [2, 18, 20, 21]. Iip10 is then converted to CLIP by proteolytic processing by CatS, CatL, CatF, or CatV, allowing for interaction with HLA-DM, peptide exchange, and ultimately, the activation of specific T cells by surface-disposed MHC II-peptide complexes [22]. Although human BLC as well as primary B lymphocytes contain active CatS and CatB, they are negative for CatL activity [7, 23–26]. Very little is known, however, about the distribution of protease activity along the endocytic route of human BLC, including possible activity variations of selected proteases at different locations. Mature CatB is present in the Ii-processing compartments in human BLC, in contrast to lysosomes [27] and has also been suggested to uniquely mark the MIIC compartment in a murine B cell line [28].

The generic inhibition of cysteine proteases using leupeptin blocks the intracellular breakdown of Ii. It arrests class II molecules in late endosomal/lysosomal compartments and impairs the endocytic transport and surface deposition of MHC class II molecules in an Ii-dependent manner, in human BLC as well as in other types of MHC II-positive cells [20, 29–31]. In most peripheral APC, such as B cells or dendritic cells (DC), elimination of CatS activity blocks conversion of Iip10 into CLIP and results in impaired peptide loading and class II function [7, 32]. Facultative APC, such as human myoblasts stimulated with interferon-γ (IFN-γ), by contrast, do not rely on CatS activity for elimination of Iip10 [33]. Further studies with murine and human DC demonstrated that the conversion of Iip10 into CLIP regulates the egress of class II to the cell surface: Immature DC containing lower CatS activity, and mature DC from CatS-deficient mice accumulated newly synthesized class II complexes attached to Iip10 in lysosomal compartments [34, 35]. Although this suggests that DC rely on the generation of CLIP for the surface delivery of class II, it is presently unknown whether such conversion of Iip10 is similarly required in APC other than DC or to what extent this may be a cell-specific, regulatory mechanism of DC, whose endocytic compartment undergoes major morphological changes unlike any other type of APC during activation [36, 37].

We here use activity-based chemical probes in conjunction with subcellular fractionation to dissect the subcellular pattern of cathepsin activity along the endocytic route of human BLC and relate it to the maturation and subcellular transport of MHC II. Our data demonstrate that individual patterns of cathepsin activity are present in different endocytic compartments and suggest that the transport of newly synthesized class II molecules to the plasma membrane of human BLC is independent from the conversion of Iip10 into CLIP by CatS.

MATERIALS AND METHODS

Cells, antibodies, and proteases

DC were generated from adherent monocytes in vitro using granulocyte macrophage-colony stimulating factor and interleukin-4 [36]; primary human B lymphocytes were isolated from buffy coats using CD22-specific magnetic beads (Miltenyi Biotec, Auburn, CA), according to the manufacturer's advice. The human BLC lines WT51 and Yesthom (homozygous for DRB1*0401) were cultured in complete RPMI-1640 medium [10% fetal calf serum (FCS); 70 μg/ml gentamycin].

Anticathepsin antisera were generated by E. Weber against recombinant cathepsins; anti-rab5 and -rab7 antibodies were generated by immunizing rabbits with appropriate peptides followed by affinity purification. The polyclonal serum against protein disulfide isomerase (PDI) was a gift from Hidde L. Ploegh (Harvard Medical School, Boston, MA). The rabbit anticystatin C (anti-CysC) antiserum was purchased from Upstate Biotechnologies (Lake Placid, NY). The sheep antiserum against AEP was a generous gift from Colin Watts (University of Dundee, UK).

Western blot

Cells/fractions lysed in Nonidet P-40 (NP-40)/pH 7 lysis buffer (50 mM sodium acetate, 5 mM $MgCl_2$, 0.5% NP-40) were resolved by 12.5% sodium dodecyl sulfate-polyacrylamide gel electrophoresis (SDS-PAGE), transferred to polyvinylidene difluoride membrane (Millipore, Bedford, MA), blocked, and probed with appropriate dilutions of the respective primary antibody, followed by a secondary anti-rabbit immunoglobulin G antibody coupled with peroxidase (Southern Biotech, Birmingham, AL). An enhanced chemiluminescence detection kit (Amersham Pharmacia, Little Chalfont, UK) was used to visualize the antibody-reactive proteins.

Active site-directed labeling

JPM565 was synthesized essentially as described [38, 39]. Radioiodination was achieved using the iodogen method (Pierce, Rockford, IL), according to the manufacturer's advice using a disposable C18 matrix (Waters) for purification [34]. Enriched, subcellular fractions were lysed in NP-40/pH 5 lysis buffer (50 mM sodium acetate, 5 mM $MgCl_2$, 0.5% NP-40) and analyzed for protein concentration using the Bio-Rad (Hercules, CA) Bradford reagent. Lysates were incubated with 1 mM ^{125}I-JPM-565 for 1 h at 37°C. Reactions were terminated by addition of SDS-reducing sample buffer and immediate boiling. Samples were resolved by 12.5% SDS-PAGE gel and autoradiography [26].

Metabolic labeling

Equal numbers of BLC were incubated in 1 ml methionine/cysteine (Met/Cys)-free medium supplemented with 10% FCS, 2 mM L-glutamine, penicillin (1:1000 dilution U/ml), and 100 mg/ml streptomycin for 30 min. Cells were pulsed for 30 min with 0.5 mCi/ml ^{35}S Met/Cys (80/20, Pharmacia, Uppsala, Sweden) and chased in 15 vol complete RPMI supplemented with FCS, L-glutamine, penicillin, and streptomycin as above for the times indicated. N-Morpholinurea–leucine–homophenylalanine–vinylsulfone-phenol (LHVS; synthesized as published in ref. [40]) was added to the pulse medium (20 min before the addition of ^{35}S Met/Cys) and the chase medium at a final concentration of 10 nM.

Subcellular fractionation

Subcellular fractions were prepared and characterized exactly as described [34, 36, 41]; all steps were performed at 4°C. At each time-point, cells were washed with phosphate-buffered saline (PBS) and 0.25 M sucrose, taken up in 2.2 ml homogenization buffer (0.25 M sucrose, 1 mM EDTA, pH 7.4, 1 mM phenylmethylsulfonyl fluoride), homogenized by six passes in a ball-bearing homogenizer (10 μm gap), and spun at 1000 *g* for 10 min to obtain postnuclear supernatants (PNS). A 27% Percoll (Pharmacia) solution (9 ml) in 0.25 mM sucrose was layered on top of a 1-ml cushion of 2.5 M sucrose and overlaid with 2 ml PNS (containing equal amounts of total incorporated radioactivity for each individual sample, as described). After 1 h centrifugation at 34,000 *g* (4°C), 1 ml fractions were collected from the bottom of the tube. Fractions containing the low-density peak of N-acetyl-glucosaminidase (NAG) activity (fractions 9 and 10) were pooled, applied to a 10% Percoll gradient, and fractionated by centrifugation as described for the 27% gradient. After fractionation, organelles were recovered by 100,000 *g* for 10 min.

Crude endocytic fractions for visualization of total protease content were generated from postnuclear supernatants by ultracentrifugation [42].

Characterization of subcellular fractions

For untreated or LHVS-treated BLC, the first gradient (27% Percoll) yielded two peaks of activity of the endocytic marker enzyme NAG (high-density peak: fractions 1+2, referred to as peak A). To distinguish between early and late endosomal compartments, the low-density peak of the NAG activity in the 27% Percoll gradient was applied to a subsequent 10% Percoll density gradient. This separation resulted in a predominant intermediate density peak of NAG activity at the bottom of the gradient, peak B (fractions 1+2 of the 10% gradient). Peak C (fractions 11+12) was defined based on distribution of protein, although a small amount of NAG activity was detected reproducibly. The marker profile showed that peak A contains mature lysosomes, based on its density of 1.09 g/ml, its NAG activity, and the presence of the late endosomal/lysosomal marker CatD. Nonlysosomal characteristics [the endosomal markers rab5 and rab7; the endoplasmic reticulum (ER) marker PDI] were absent from peak A. The intermediate density peak of the 10% Percoll gradient (peak B) represents late endosomes (density 1.05 g/ml, positive for NAG, accumulation of rab7). The low-density peak (peak C) consists of a mixture of compartments, namely ER/Golgi and early endosomes, in agreement with published observations [43]. For every fraction of each individual experiment, the distribution of the endocytic marker NAG was assayed as described [42].

Immunoprecipitation

Immunoprecipitation experiments were performed exactly as described [34].

Cell-surface biotinylation and immunoprecipitation

BLC labeled in a pulse-chase experiment were washed three times in ice-cold PBS and incubated for 30 min at 4°C in PBS containing 0.5 mg/ml NHS-Sulfo-Biotin (Pierce). For each time-point, the biotinylated cells were lysed in NP-40 lysis buffer, and class II molecules were immunoprecipitated with the Tü36 antibody. Staph A pellets were resuspended in 50 μl PBS containing 1% SDS and boiled 10 min. One-tenth of each precipitate was retained for later comparison with reimmunoprecipitates in SDS-PAGE. Lysis buffer (1 ml) containing 0.1% bovine serum albumin was added to the remaining nine-tenth of the precipitate. After centrifugation, the supernatant was precleared once, reimmunoprecipitated with streptavidin-agarose beads as above, and analyzed by SDS-PAGE.

Isolation and identification of labeled polypeptides

Cell lysates from bulk cultures of BLC were incubated with 5 μM DCG04, a biotinylated derivative of JPM565, which shows a virtually identical labeling specificity and allows direct retrieval of the labeled polypeptides, as published [13]. As control, a parallel sample was heated to 95°C 5 min before labeling to functionally inactivate proteases. After elimination of excess DCG04 using a PD-10 column in the presence of SDS 0.5%, DCG04-labeled polypeptides were purified with streptavidin-sepharose beads, followed by extensive washing, as described [13]. The polypeptides retrieved were resolved by SDS-PAGE and visualized by staining with colloidal Coomassie. A small-size, 10 × 10 cm, commercial minigel format was necessary to be able to visualize the limited amounts of protein retrieved, which shows a lower degree of resolution in the 25–35 kD range, compared with the larger size gels (35×25 cm) used in all other experiments.

To identify the visualized polypetides, in-gel digestion was performed as described [44] with minor modifications. The protein bands of interest were excised from the gel and washed with Millipore-purified water and with 50% acetonitrile/water. After drying, trypsin (sequencing grade, Promega, Mannheim, Germany) was added to the sample. Tryptic protein fragments were sequentially extracted from the gel matrix using 5% formic acid and 50% acetonitrile/5% formic acid. The extracts were pooled and concentrated in a speed vac concentrator. After purification using ZipTips (C18-ZipTip, Millipore), aliquots were deposited on spots of α-cyano-4-hydroxycinnamic acid/nitrocellulose and were analyzed using a Reflex III matrix-assisted laser desorption ionization-time-of-flight mass spectrometer (MALDI-TOF-MS; Bruker Daltonic, Bremen, Germany). The sequences of peptides were analyzed using nanoelectrospray tandem MS on a hybrid quadrupole orthogonal acceleration TOF MS (QSTAR Pulsar i, Applied Biosystems/MDS Sciex, Foster City, CA), equipped with a nanoflow electrospray ionization source and nanoelectrospray needles (BioMedical Instruments, Zoellnitz, Germany). The instrument was calibrated externally. Tandem mass spectra were obtained by means of collision-induced decay of selected precursor ions.

Database searches (NCBInr) were performed using the MASCOT software from Matrix Science (Beachwood, OH) [45] with methionine oxidations as variable modifications based on a probability value of $P < 0.05$. The following peptide masses are all given in the monoisotopic 1+ protonated form.

CatC

Two relevant peptide masses of 1053.56 Da and 1338.71 Da were detected using peptide mass fingerprinting. The sequence of the 1338.71 Da peptide was clearly determined as NVHGINFVSPVR, derived from CatC. In addition, we also detected the y_4, y_5, and y_6 ions of the 1053.56 Da peptide of the CatC-derived sequence GIYHHTGLR.

CatH

A peptide mass fingerprint of CatH (masses of 1089.58 Da, 1356.70 Da, 1458.63 Da, 1474.62 Da, and 1797.95 Da) was found by MALDI analysis. Sequencing of the 1089.58 Da peptide revealed the sequence NGIPYWIBK, the 1797.95 Da peptide revealed the partial sequence . . . VNHAVLAVGY-GEK, and the 1458.63 Da peptide revealed the sequence GIMGEDTY-PYQGK, all of which are derived from CatH.

CatS

The peptide masses 998.50 Da, 1066.55 Da, and 1357.68 Da were found using peptide mass fingerprinting, indicating the presence of CatS. Sequencing the 998.50 Da peptide resulted in the sequence YTELPYGR, and a 956.50 Da peptide resulted in the sequence GPVSVGVDAR, both derived from CatS.

RESULTS

Subcellular distribution of cathepsins in the endocytic tract of human BLC

To dissect the endocytic pathway of BLC on a subcellular scale, we subjected postnuclear supernatants of BLC to a

stepwise fractionation procedure that has previously been used to discriminate among lysosomes, late endosomes/MIIC, and early endosomal compartments in B cells/BLC and DC [34, 36, 43, 46]. Briefly, postnuclear supernatants were first separated by a 27% Percoll gradient, which separated a dense fraction (peak A) from the remaining material. This unresolved portion was applied to a subsequent 10% Percoll gradient, which again resulted in a dense fraction (peak B) and unresolved material on top of the gradient (peak C). Consistent with earlier data, peak A was enriched for NAG activity and CatD (**Fig. 1, a** and **b**), identifying it as lysosomal material, and peak B contained NAG and rab7, consistent with its late endosomal characteristics. In peak C, rab7 was present only in minute amounts, whereas rab5 was continuously detected in low-density frac-

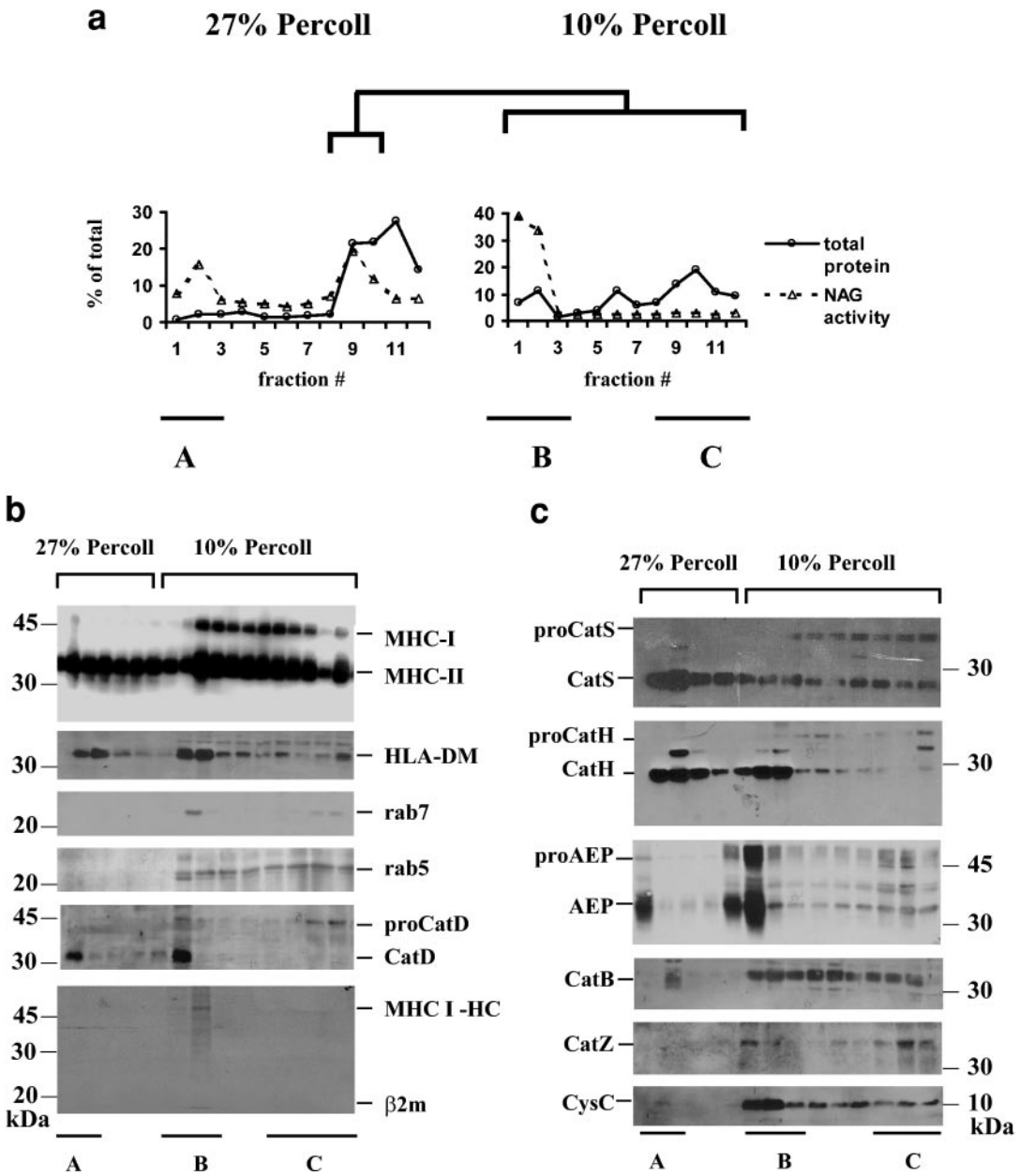

Fig. 1. (a) Distribution of endocytic marker proteins in subcellular fractions. Postnuclear supernatants from BLC were resolved on two consecutive Percoll gradients as described, yielding three peaks of NAG activity and protein content, respectively (A–C). Results are expressed in percent of total of each gradient. (b) Subcellular distribution of MHC I and II and endocytic marker proteins. Subcellular fractions (a) were analyzed for the distribution of MHC classes I and II as well as HLA-DM and the endocytic marker rab5 (early endosomes), rab7 (late endosomes), and CatD (late endosomes and lysosomes) under steady-state conditions by immunoblot using equal volumes from each subcellular fraction (top five panels). To asses the localization of cell-surface-derived proteins within the fractionation scheme, MHC I complexes were selectively retrieved from the plasma membrane after surface biotinylation of cellular protein and sequential immunoprecipitation with W6/32 and StaphA followed by streptavidin–sepharose (bottom panel). The signal obtained after autoradiography selectively represents MHC class I molecules (HC, heavy chain; β2m, β-2-microglobulin) retrieved from the plasma membrane. (A–C) Major activity peaks referred to as lysosomes (A), late endosomes/prelysosomes (B), and early endosomes (C) in good agreement with the published characteristics of the method. (c) Subcellular distribution of cathepsins and their inhibitors. Subcellular fractions (a) were probed by immunoblot using appropriate antisera against cathepsins, AEP, and CysC, respectively, to assess the steady-state distribution of CatS, CatH, AEP, CatB, CatZ, and CysC. Equal volumes from each subcellular fraction were assayed.

tions, demonstrating that early endosomal material cofractionated in peak C, in agreement with published data. To relate the distribution of cell-surface-derived molecules to this fractionation scheme, BLC were pulse-labeled with ^{35}S Met/Cys for 30 min at 37°C, followed by a 1-h chase in the presence of excess cold Met/Cys. Cells were then transferred on ice for 30 min, followed by biotinylation of cell-surface molecules as described. Subsequently, cells were subjected to the fractionation protocol and lysed, and total MHC class I complexes were retrieved from individual fractions by immunoprecipitation. After elution of the bound material from StaphA, the biotinylated (and surface-exposed) fraction of MHC I was reimmunoprecipitated using streptavidin-sepharose beads, followed by resolution by SDS-PAGE and autoradiography. In contrast to total class I (top panel, visualized by Western blot), surface class I was exclusively retrieved from peak B. Thus, although the fractionation procedure enriched lysosomal (peak A), late endosomal (peak B), and early endosomal material (peak C) in distinct fractions, it did not separate plasma membrane-derived protein from endosomal compartments.

During steady-state, MHC II was present in roughly equal amounts throughout all fractions, consistent with its abundant presence in lysosomes, endosomes, and at the plasma membrane, respectively, as assessed by immunoblot. In contrast, MHC I was absent from peak A, demonstrating that sizable amounts of MHC I do not reach conventional lysosomes in BLC. HLA-DM, the catalyst for MHC II-peptide loading, was enriched in peak B but was also significantly present in peak A and detectable in peak C. This suggested that MHC II peptide exchange is concentrated in late endosomal and to a lesser extent, lysosomal compartments but may also be found along the entire endocytic route.

As cathepsins are involved in the generation of substrates for HLA-DM (conversion of Ii into CLIP as well as degradation of complex protein into antigenic peptide), we tested whether these proteases would follow the same subcellular distribution as HLA-DM (Fig. 1c). CatS was mainly detected in lysosomal fractions (peak A); however, significant CatS protein was present in late endosomes and throughout the entire endocytic pathway of BLC. Its zymogen, proCatS, was absent from lysosomes, suggesting that activation of cathepsins from its proform was located upstream in endosomal compartments. CatH, by contrast, more closely matched the subcellular distribution of HLA-DM. It was equally distributed between lysosomes and late endosomes, whereas early endosomes contained very little CatH. Similar to proCatS, proCatH was detected in early and late endosomes, implicating activation of CatH from its proform preferentially in late endosomes. The AEP followed this distribution pattern, i.e., conversion from the zymogen in late endosomes and presence of the mature polypeptide in late endosomes and lysosomes, although its lysosomal representation was significantly lower than the amount of AEP detected in late endosomes. The distribution patterns of CatB and CatZ were distinct from that observed for CatS, CatH, and AEP as well as HLA-DM: Only trace amounts of CatB were present in lysosomes. Instead, the majority of mature CatB polypeptide was found in late and early endosomes. A similar pattern was observed for the mature form of CatZ. CysC, the main endogenous inhibitor of cathepsin activity, was distributed very similarly to CatZ and CatB and concentrated in peak B while being absent from lysosomes.

In summary, the main papain cathepsins and their major inhibitor followed two different patterns of subcellular distribution in BLC: Although CatS, CatH, and AEP cofractionated with HLA-DM in late endosomes and lysosomes, CatZ and CatB as well as CysC were absent from lysosomes but were found not only in late endosomes but also in early endosomal fractions in significant amounts. This suggested that the pattern of protease activity may also change along the endocytic pathway.

Subcellular distribution of cathepsin activity in human BLC

Cathepsin activity cannot be deduced from the mere presence of the mature polypeptide but relies on the complex interaction of zymogen activation, subcellular transport, the presence/absence of endogenous inhibitors, as well as redox potential and pH. Activity-based, active site-directed chemical probes are being increasingly used to assess the presence of active proteases in complex protein mixtures [38]. JPM565 is an E64 derivative that covalently binds to the active-site cysteine of papain-like cysteine proteases via its epoxide function. Its radioiodinated version ^{125}I-JPM565 represents an established tool to visualize active cathepsins after incubation of cellular extracts with the probe, SDS-PAGE, and autoradiography. As we have recently demonstrated by immunoprecipitation of the labeled polypeptide species, ^{125}I-JPM565 visualizes CatS, CatH, and CatB in human BLC in an activity-based manner [26]. To directly compare the activity levels of these enzymes between BLC and primary human B cells and to relate it to those in other types of professional APC, crude endocytic extracts from either type of cell were incubated with the probe, and active cathepsins were visualized by SDS-PAGE and autoradiography (**Fig. 2a**, upper panel). Consistent with earlier results, BLC contained significant amounts of active CatH as well as CatS in smaller quantities. Although sizable amounts of the CatB polypeptide were detectable by Western blot (see above), this translated into only trace amounts of active CatB, as deferred from activity-based labeling. Two additional, as-yet unidentified activity signals were detected at ~25 and 37 kD, as published [26]. They both represent papain-like cysteine proteases, as labeling can be inhibited by prior exposure to E64 (data not shown), but they are not reactive with antisera against CatS, -L, -B, -H, and -Z [26]. Except for the 25-kD active polypeptide, freshly isolated, human peripheral blood B lymphocytes contained a similar activity pattern for cathepsins as BLC: The dominant activity was CatH (together with the 37-kD polypeptide), active CatS was present to a lesser extent, and only traces of CatB activity could be detected in this type of cell.

To reveal the identity of this 25-kD signal, BLC-derived cell lysates were incubated with the biotinylated JPM565 derivative DCG04 along with a control sample that had been heated to 95°C before labeling to functionally inactivate the polypeptides. The labeled species were retrieved using streptavidin beads (Fig. 2a, lower panel) and identified after excision and in-gel digest by MS [13]. Three prominently labeled species in the 25- to 35-kD range were isolated, as expected. The absence

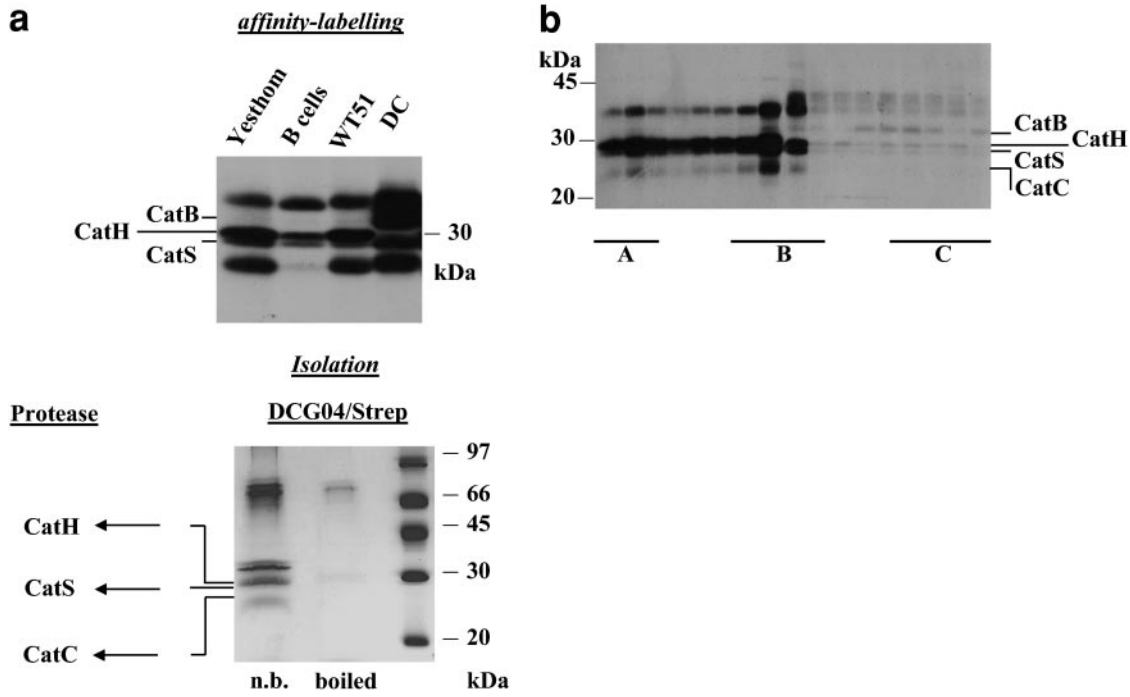

Fig. 2. (a) Upper panel: Visualization of active cathepsins in BLC and primary human B lymphocytes. Active cathepsins in crude endocytic extracts from BLC (Yesthom, WT51), freshly isolated human peripheral blood B lymphocytes (B cells), and monocyte-derived human DC were labeled with ^{125}I-JPM-565 and analyzed by SDS-PAGE and autoradiography. Lower panel: Identification of active cathepsins in BLC. Whole cell lysates from BLC were incubated with the biotinylated JPM565 derivative DCG04, followed by retrieval of the labeled species using streptavidin-sepharose beads. For specificity control, a parallel sample was heated to 95° (boiled) before labeling. After resolution of the retrieved polypeptides and Coomassie staining, the indicated polypeptides were excised, digested with tyrpsin, and identified as the CatS, -H, and -C by MS, as described in Materials and Methods. n.b., Nonboiled. (b) Subcellular distribution of active cathepsins in human BLC, which were subjected to subcellular fractionation as described, and equal volumes from each fraction were incubated with ^{125}I-JPM-565 and analyzed by SDS-PAGE and autoradiography. The endocytic compartments resolved are A, lysosomes; B, late endosomes/MIIC together with plasma membrane; and C, early endosomes.

of these polypeptides in the boiled sample confirmed the specificity of labeling and the isolation procedure. MS identified the 25-kD signal as CatC, and the 30-kD signal contained CatS and CatH, as detailed in Materials and Methods. The 37-kD signal contained a mixture of polypeptides that we could not unequivocally identify on this 1-D level of resolution. Further refinement of the isolation protocol allowing retrieval of sufficient amounts of protein for use with 2-D SDS-PAGE will be necessary to identify the additionally labeled polypeptides at 37 kD.

When subcellular fractions derived from BLC were labeled with the activity-based probe, we observed distinct distributions of active cathepsins along the endocytic pathway (Fig. 2b): The vast majority of cathepsin activity was concentrated in late endosomal and lysosomal compartments. However, consistent with the distribution of the CatB polypeptide, active CatB preferentially cosedimented with early endosomal fractions, where its relative activity was in the same order of magnitude as that of the other activity signals detected, and it was absent from lysosomes. By contrast, active CatS and CatH were distributed evenly between lysosomal and late endosomal compartments. The 37-kD activity signal as well as CatC were preferentially found in the late endosomal peak B but were also significantly present in the lysosomal fractions A. Thus, the pattern of active papain cathepsins gradually changed along the endocytic tract of BLC: Lysosomes contained a protease panel that was qualitatively distinct from that found in early endosomes, and the proteolytic machinery in late endosomes combined the content of lysosomal and early endosomal compartments.

Role of CatS for Ii processing and the intracellular trafficking of MHC II in human BLC

Having dissected the subcellular pattern of cathepsin activity and class II-related molecules under steady-state conditions in BLC, we next analyzed the maturation and transport of MHC class II molecules along this cellular pathway. In particular, we asked whether CatS activity was essential for Ii processing, conversion of Iip10 into CLIP, and the regulation of distribution and export of class II in human BLC, similar to the situation known from murine DC [35]. To this end, we performed metabolic labeling of BLC in the presence or absence of LHVS (10 nM), which selectively eliminates CatS activity in this concentration range [7, 23, 33, 47], followed by pulse-chase analysis and immunoprecipitation of class II. MHC II complexes were retrieved with the conformation-specific Tü36 antibody and analyzed by SDS-PAGE and autoradiography under strongly denaturing (boiled) or mildly denaturing (non-boiled) conditions to account for individual polypeptides present in class II complexes or for the formation of stable, mature αβ-peptide (αβp) complexes that are resistant to SDS at room temperature [48].

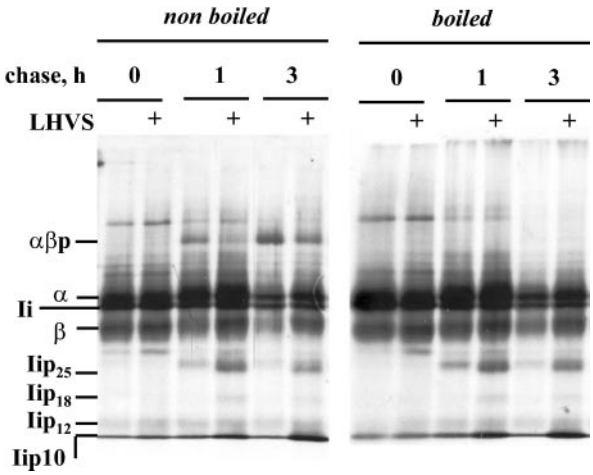

Fig. 3. Maturation of MHC II and Ii processing in the absence of CatS activity in human BLC, which were pulse-labeled with ^{35}S Met/Cys for 30 min, followed by a chase for up to 3 h, in the presence or absence of the selective CatS inhibitor LHVS (10 nM). After lysis, class II complexes were retrieved by immunoprecipitation using the conformation-specific Tü36 antibody. SDS-PAGE at room temperature (non boiled) or after prior exposure to 95° (boiled) followed by autoradiography allowed to account for fully mature class II αβp complexes, the individual, full-length polypeptides (α, β, Ii), as well as degradation products of Ii of the indicated molecular weight (Iip_{25}, Iip_{18}, Iip_{12}, Iip10).

When BLC were pulse-labeled with ^{35}S Met/Cys for 30 min and chased for 1 h or 3 h, respectively, in the presence or absence of LHVS (10 nM), the pattern of the labeled MHC II complexes after immunoprecipitation with Tü36 was essentially as published [7, 34] (**Fig. 3**): Inhibition of CatS interfered with the efficient formation of SDS–stable class II αβp complexes (nonboiled samples) and led to the accumulation of Ii processing intermediates at 25, 18, 12, and 10 kD (Iip25–Iip10). However, unlike the results obtained in the murine system [34], inhibition of CatS activity did not prevent the formation of SDS–stable mature αβp complexes but only reduced the efficiency of their generation, and mature αβp complexes were detected in significant amounts in the LHVS-treated sample after 3 h of chase. It is important that the total amount of Iip10 retrieved continued to increase from the 1-h to the 3-h chasepoint, confirming that conversion of Ip10 into CLIP was continuously inhibited by LHVS. This implicated that mature αβp complexes can be formed without efficient conversion of Iip10 into CLIP in BLC, suggesting that HLA-DM may also interact with Ip10 instead of CLIP for peptide exchange in human APC.

To dissect the role of CatS activity during Ii processing in human BLC on a subcellular scale, we performed metabolic labeling/pulse-chase experiments in the presence/absence of CatS activity as above, chased for 1 h and 3 h, respectively, and at each chasepoint, subjected the cells to the subcellular fractionation procedure described in **Figure 4**. After 1 h, the results obtained in the presence or absence of CatS activity (+LHVS 10 nM) were virtually identical: Class II complexes were almost evenly distributed over the 10% percoll gradient, consistent with their location in the ER/Golgi, in endosomal compartments, and at the cell surface, respectively, and lysosomes contained virtually no class II. Ii processing products (namely Iip10) were detectable in small but comparable quantities, in particular, in late endosomal fractions. Upon 3 h of chase in the absence of LHVS (left panels), sizable amounts of class II had reached the lysosomal compartment. These were devoid of intact Ii or its degradation intermediates, demonstrating that the bulk of Ii processing had been completed upstream from lysosomes. Consistent with this interpretation, Iip10, the substrate for CatS, was mostly detected in the late endosomal peak B, and only traces were present in the lysosomal compartment A. Analysis of the same samples without prior boiling revealed that the vast majority of lysosomal MHC class II was present in the mature, SDS–stable II αβp formation, and all other subcellular locations contained significant amounts of immature class II complexes that dissociated into their individual polypeptide chains during SDS-PAGE at room temperature. Thus, the bulk of fully mature SDS–stable class II complexes is formed before class II complexes reach the lysosomal compartment.

When BLC were exposed to LHVS during pulse-chase analysis (Fig. 4, right panels), immunoprecipitation with Tü36 from individual, subcellular fractions at the 3-h chasepoint revealed the subcellular distribution of Ii processing intermediates: Iip12 and Iip10 accumulated in different relative ratios along the endocytic route, in good agreement with the differential, subcellular distribution of protease activity in endocytic compartments. Although Iip12 was more prominent than Iip10 in fractions cosedimenting with early endosomes, both intermediates were present in similar amounts in the late endosomal peak B, and Iip10 was preferentially found in lysosomes. Given that Iip10 and Iip12 contain the intact, N-terminal, cytoplasmatic tail of Ii [47], this suggests that C-terminal processing of Ii is performed at different positions within the C-terminal

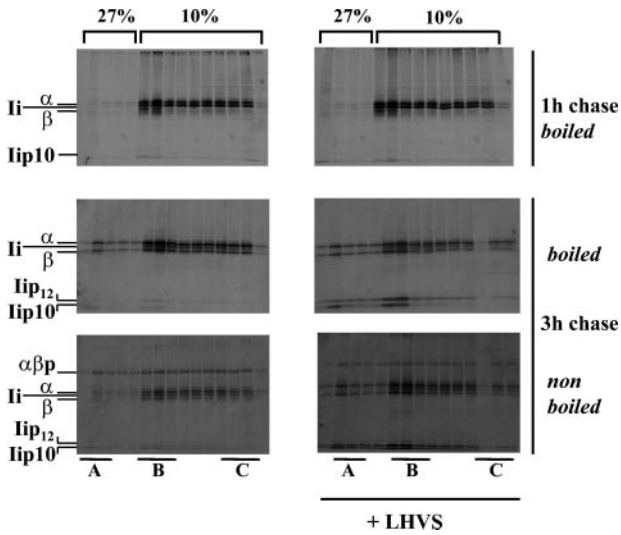

Fig. 4. Subcellular transport of class II in the absence of CatS activity. BLC were pulse-labeled and chased in the presence/absence of LHVS (10 nM) as before and subjected to subcellular fractionation at each chasepoint, followed by immunoprecipitation of class II complexes from each fraction using Tü36, SDS-PAGE, and autoradiography. Although addition of LHVS resulted in the accumulation of Iip10 at the 3-h chasepoint, it did not change the intracellular distribution of class II. αβp, Fully mature class II αβp complexes. (A–C) The major endocytic fraction lysosomes (A), late endosomes/MIIC (B), and early endosomes (C).

portion of Ii, generating Ip10 or Ip12, depending on the subcellular compartment where processing occurs.

When comparing the relative distribution of class II β chain between the LHVS-treated and the nontreated fractions at the 3-h time-point, no influence of CatS activity on the subcellular distribution of class II complexes was observed. In particular, unlike the situation described for murine DC, elimination of CatS activity did not lead to an accumulation of class II complexes in lysosomal compartments. To address the subcellular distribution of SDS–stable class II dimmers, we analyzed the same samples under mildly denaturing conditions. Again, formation of SDS–stable dimers in general was more efficient when CatS activity was present; however, absence of CatS activity did not block the formation of these complexes. It is important that their relative subcellular distribution was not affected by changes in CatS activity (c.f., the results obtained in the presence or absence of LHVS at the 3-h chasepoint). In summary, these data suggested that the continued presence of Iip10 in class II complexes did not affect the intracellular distribution of class II in human BLC, in contrast with DC. This implicates that CatS activity and the conversion of Iip10 into CLIP are of minor importance for the control of intracellular class II transport in human BLC. Consequently, the mechanism that controls the egress of class II from endocytic fractions in human BLC might also be distinct from that found in murine DC.

CatS activity is dispensable for efficient surface delivery of MHC II in human BLC

To selectively account for newly formed class II complexes that have been delivered to the plasma membrane, we combined metabolic labeling with surface biotinylation at different chase-points, followed by sequential immunoprecipitation with Tü36 and streptavidin beads. To control for the specificity of immunoprecipitation with streptavidin–sepharose, we pulse-labeled BLC for 30 min, followed by a 3-h chase. The sample was split, and one-half was surface-biotinylated at 4°, followed by lysis and immunoprecipitation of both samples using the Tü36 antibody. Of the retrieved material, 10% was loaded on the gel (total), and the remaining 90% was dissociated from StaphA by boiling in SDS, followed by a second round of immunoprecipitation using streptavidin-sepharose beads, followed by SDS-PAGE and autoradiography (**Fig. 5a**, left panel). Although identical amounts of class II were retrieved from the total lysate of biotinylated/nonbiotinylated cells, the reprecipitation using streptavidin beads specifically precipitated class II molecules from the biotinylated sample, confirming that the reprecipitation with streptavidin–sepharose was highly selective for biotinylated protein. To exclude that intracellular protein was nonspecifically biotin-modified during surface biotinylation, BLC were pulse-labeled, chased for 3 h, and surface-biotinylated as before. The ER-resident PDI was retrieved from the samples by immunoprecipiation using an appropriate serum. Again, 10% of the retrieved material was directly loaded on the gel (total), and the remaining 90% was subjected to a second round of immunoprecipitation using streptavidin-sepharose beads (surface). Analysis of the samples by SDS-PAGE and autoradiography revealed that PDI was not retrieved by streptavidin–sepharose, confirming the cell-surface selectivity of biotin treatment and sequential immunoprecipitation (Fig. 5a, left panel).

To address the presence of newly synthesized class II dimers on the cell surface, we performed pulse-chase analysis type of

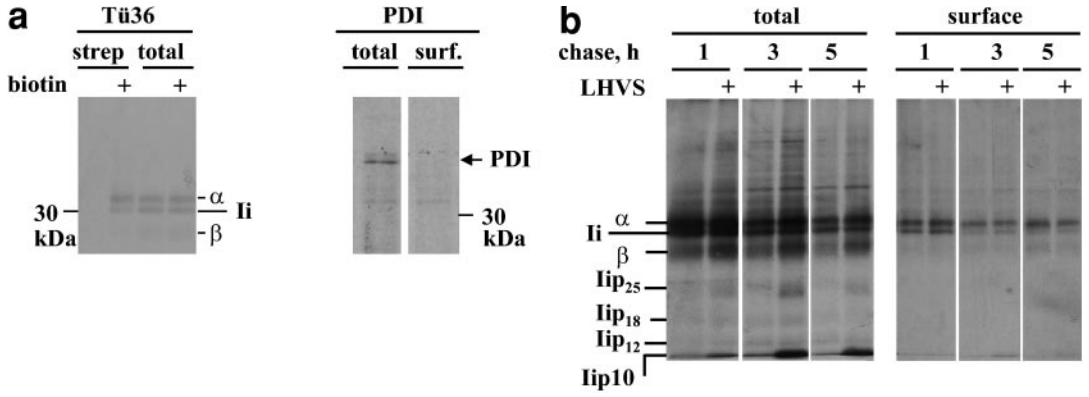

Fig. 5. (a) Selectivity and specificity of surface biotinylation and retrieval of biotinylated proteins. (Left) To demonstrate the specificity of biotinylation and the retrieval of biotinylated protein by consecutive immunoprecipitation with streptavidin beads, one-half of the sample was surface-biotinylated (+biotin) after metabolic labeling and a 3-h chase. Total class II complexes were retrieved with Tü36 from both portions, 10% of each precipitate was loaded on the gel (total), and the remaining 90% was subjected to a second round of precipitation using streptavidin-sepharose beads (strep). Only in the biotinylated sample, class II was visualized after this second immunoprecipitation. (Right) To demonstrate that intracellular molecules are not accidentally retrieved by the method, BLC were pulse-labeled and chased for 3 h, followed by surface biotinylation. The ER-resident chaperon PDI was immunoprecipitated, 10% of the total precipitate was subjected to SDS-PAGE (total), and the remainder underwent a consecutive immunoprecipitation using streptavidin sepharose (surf.). Analysis by SDS-PAGE and autoradiography revealed that surface biotinylation did not biotin-modify intracellular PDI. (b) Delivery of class II to the cell surface in the absence of CatS activity. BLC were pulse-labeled with ^{35}S Met/Cys as described and chased for the times indicated, in the presence or absence of LHVS 10 nM. At each chasepoint, cells were surface-biotinylated as described and lysed, and total class II complexes were immunoprecipitated using Tü36 and StaphA. The precipitate (10%) was analyzed by SDS-PAGE under fully denaturing conditions (total, left panel). The remaining portion was released from StaphA and reprecipitated using streptavidin-sepharose beads to account for that portion of total class II that had newly reached the plasma membrane after the pulse (surface, right panel). Precipitates were visualized by autoradiography after SDS-PAGE.

experiments in conjunction with biotinylation of extracellular protein at each chasepoint (1 h, 3 h, 5 h), followed by retrieval of class II by immunoprecipitation with Tü36. The precipitated material (10%) was directly loaded on the SDS gel (Fig. 5b, total, left panel), and surface-exposed MHC II was specifically isolated from the remaining 90% by sequential immunoprecipitation with streptavidin-sepharose beads (surface, right panel). The effect of LHVS on the processing of total cellular MHC II complexes was essentially identical to that seen in Figure 3 as well as to published data: LHVS induced the accumulation of Ii processing intermediates, in particular Iip10, which reached maximum quantities at 3 h of chase. At the cell surface, newly synthesized class II complexes were present at 1 h of chase in the absence of LHVS, predominantly representing the fraction that reaches endocytic compartments via the plasma membrane. Consistent with this, we observed similar signal intensities for the class II α chain and intact Ii, indicating that most of the complexes retrieved contained intact Ii and had not yet undergone proteolytic processing. Upon 3 h of chase, the intensity of surface class II signals decreased, suggesting that internalization of newly synthesized class II quantitatively exceeded class II export in this period of time. Note that the relative intensity of the Ii signal retrieved from the cell surface decreased after 3 h of chase compared with the 1-h time-point. This contrasted with the relative ratios observed with total cellular class II (left panel) at this time-point, where this ratio remained largely constant, indicating that class II complexes that had undergone Ii processing in the endocytic compartment have been exported to the plasma membrane after 3 h of chase. After 5 h, the amount of newly synthesized class II retrieved from the cell surface increased relative to the 3-h time-point, and the proportion of intact Ii further decreased. In summary, these data are consistent with the interpretation that a major portion of newly synthesized class II, which was present at the cell surface after 1 h of chase, was on its transit from the plasma membrane to endosomal compartments for Ii processing and peptide-loading, in agreement with published data [48]. At 3 h and 5 h of chase, the majority of radiolabeled surface class II represented a pool of class II complexes that had been exported form the endocytic compartment after completion of Ii processing.

Comparison of the LHVS-treated/nontreated samples at the 3 h and 5 h chasepoints revealed that the total amount of radiolabeled α or β chain at the cell surface was not influenced by LHVS treatment, demonstrating that CatS activity neither affected the kinetics nor the quantities of class II export to the plasma membrane in human BLC. Of note, a small amount of Iip10 could be retrieved in complex with class II from the cell surface from LHVS-treated BLC at the 3-h chasepoint. This not only confirmed the efficiency of CatS inhibition by LHVS in this sample but suggests that the continued association of Iip10 with class II αβ dimers did not prevent transport of class II complexes to the plasma membrane in this type of cell. Thus, although CatS activity is required for Ii processing, it is dispensable for normal intracellular transport and surface delivery of MHC II complexes in human BLC.

DISCUSSION

Cathepsin activity is considered a major regulatory switch in the class II antigen-presentation pathway. As both proteolytic pathways involved (processing of Ii and antigen) rely on limited proteolysis rather than complete peptide destruction, a highly regulated, proteolytic environment appears mandatory in class II antigen-processing compartments [1, 12]. The low-substrate specificity of cathepsins per se is unlikely to sufficiently provide an environment that allows for limited proteolysis and the survival of 9–20 mer peptides that are ultimately loaded on class II; therefore, other regulatory mechanisms for limiting proteolytic turnover are likely to exist. The cellular microarchitecture of class II-positive endocytic compartments consists of a variety of specialized endocytic vesicles that gradually transit from the cell biological correlates of early endosomes to late endosomes and lysosomes [14, 15, 27, 49]. We know relatively little about the subcellular activity of cathepsins and their regulation in APC. Given that individual cathepsins differ in their pH optima and that conditions such as pH and redox potential are likely to change along this endocytic pathway, differential activity of cathepsins in different endocytic compartments might be expected, which would allow for a stepwise, rather than complete, destruction of protease substrates. The development of chemical tools that visualize proteases in an activity-based manner allows us to address these type of questions directly. Here, we represent a first analysis of the subcellular distribution of active cathepsins in human BLC in relation to the major constituents of the class II antigen-presentation machinery and the transport and maturation of class II molecules.

As our results demonstrate, the activity of individual endocytic proteases indeed differs among early endosomal, late endosomal, and lysosomal compartments. We observed two distinct patterns of protease activity, which overlapped in late endosomes: Although CatB and CatZ were detected in early and late endosomes but were absent from lysosomes, CatS, CatH, CatD, CatC, and AEP were located in late endosomal and lysosomal compartments and were only poorly present in early endosomes. This is at first glance surprising, given that the pH optimum for CatB in vitro is 5.5, and CatH and CatS are stable and active at near-neutral pH. However, CatB is also active at early endosomal pH in vitro, and CatS and CatH are fully functional at late endosomal/lysosomal pH (C. Driessen, unpublished observations). Furthermore, morphological as well as recent functional data are in good agreement with this finding: Exogenous material internalized by human BLC colocalized with Ii and MHC II in CatB-positive, endosomal compartments after only 2 min of chase, consistent with an early, endosomal localization of CatB in this cell type [27]. CatB was also selectively present in MIIC-like late endosomes from murine BLC but absent from lysosomes [28]. Functional data from CatB-deficient mice indicate that CatB performs the first proteolytic step after uptake of a model antigen into APC, consistent with a dominant activity of CatB in early endocytic compartments [10]. Two recent studies have analyzed the order in which phagosomes of J774 murine macrophages acquire endocytic hydrolases, on a proteomic and a functional level

[13, 50]. Although phagocytosis is not the preferred mode of antigen uptake by BLC, and the intracellular microarchitecture between phagocytes and BLC is likely to differ significantly, our data are consistent with the results described there: CatB and CatZ were acquired by phagosomes already at very early time-points, and in particular, the exposure to CatS constantly increased toward longer internalization times [13]. This is in line with the preferential, early endosomal location of CatB and CatZ found in our results as well as with the presence of active CatS in early endosomal compartments and the continued increase in CatS activity toward late endosomes/lysosomes.

These distinct, subcellular patterns of protease activity are functionally reflected by the accumulation of different relative ratios of the Ii processing intermediates Iip10 and Iip12 at various endocytic locations when CatS activity was inhibited by LHVS. As both fragments accumulated only in the absence of CatS activity, Iip12 represents a precursor for Iip10 that is converted into Iip10 by CatS via C-terminal processing, or both fragments are substrates for N-terminal turnover by CatS, generating CLIP. In either case, the differential distribution of the fragments implicates that different proteolytic steps in Ii processing are located at distinct subcellular locations in BLC. Late endosomes contained similar quantities of both fragments, in agreement with our finding that the entire spectrum of endocytic protease activity was present only in this compartment.

MIIC most likely represent the morphological equivalent of late endosomal compartments [49] and are the major location for Ii processing in human BLC [16, 18]. In agreement with these data, Ii processing was completed in late endosomes in our results, and lysosomes contained exclusively, fully mature αβp complexes. In addition, here, we show that late endosomes are abundantly equipped with all components of the proteolytic machinery of the class II pathway: They contain the entire set of active proteases (CatS, -Z, -B, -D, -H, -C, AEP), regulatory components of protease activity such as CysC and inactive zymogens, together with MHC class II and HLA-DM.

Recent results indicated that the activity of endocytic proteases not only differs between different types of APC but also between primary cells and immortalized cells lines [26]. Here, we present a first activity-based comparison of the patterns of cysteine proteases in freshly isolated, primary human B lymphocytes, BLC, and DC. Similar to human BLC, CatS and in particular, CatH are the major active proteases in the endocytic compartment of primary B cells, and active CatB is present only in minute amounts. In contrast to human BLC, active CatC was largely absent from primary B cells. CatL, by contrast, is absent from human primary B cells and BLC, as we and others have previously demonstrated [7, 23, 26]. In murine splenocytes, a similar activity-based probe visualized significant amounts of CatB and CatL in addition to CatS and CatH [10]. Thus, not only do different types of APC contain distinct panels of proteases, but also, different protease activities might be found between similar cell types from different species.

What is the function of CatS for the processing and transport of class II in BLC? Recent years have established a close connection between the subcellular transport and processing of MHC class II molecules and the activity and function of CatS and CysC, the putative endogenous inhibitor of CatS. Studies performed with mature DC lacking CatS activity or with mature and immature murine DC that regulate CatS activity in a developmental manner demonstrated that Iip10-containing class II complexes accumulated in lysosomal compartments after 3 h of chase and failed to reach the plasma membrane in a timely manner [34, 51]. Mainly from these data, it was generalized that the presence of Iip10-containing class II complexes directly regulated the intracellular transport and surface display of class II, not only in DC but in professional APC in general [2]. However, such a direct connection between the conversion of Iip10 into CLIP by CatS and class II surface delivery has not been established for APC other than DC and in particular, not in the human system. Also, the view that CatS activity controls class II surface level by regulating Iip10 conversion has been challenged: DC and splenocytes from CatS-deficient mice display the same level of surface class II compared with cells from wild-type littermates, although Iip10 accumulates in the absence of CatS activity in both cell types [32, 34]. Moreover, the regulation of total surface class II in DC might be more the net result of differential endocytic activity of mature versus immature DC and independent from changes in CatS activity during maturation [32, 34, 52], although CatS-deficient DC accumulated Iip10-containing class II complexes in late endocytic compartments and showed an impaired kinetics of class II surface delivery. Thus, DC might not represent a valid model for other types of APC to analyze the regulation of class II transport. In addition, human myoblasts down-regulated IFN-γ-induced class II expression upon inhibition of CatS activity, and no Iip10 accumulated in this cell type, also suggesting little functional connection between elimination of Iip10 and surface delivery of class II in APC [33]. However, class II transport in BLC relies on protease activity, as is well established that the general inhibition of serine and cysteine proteases using leupeptin in human and murine BLC impairs not only Ii processing but also surface delivery of MHC II, leading to the accumulation of class II–Ii complexes in late endosomal/lyosomal compartments [18, 29, 31, 53, 54].

In our results, selective inhibition of CatS and accumulation of Iip10 did not prevent formation of mature αβp complexes in human BLC during the 3-h chase but only moderately decreased its efficiency, similar to the results observed with human DC [23]. As the total amount of αβp and the quantities of labeled Iip10 simultaneously increased in LHVS-treated BLC between the 1 h and 3 h chasepoints, it is unlikely that additional, perhaps as-yet unidentified, enzymes substituted for CatS activity and converted Iip10 into CLIP in this time interval, allowing for the HLA-DM-mediated exchange of CLIP with antigenic peptide. More likely, human HLA-DM might directly interact with human Iip10 to some extent, catalyzing formation of the mature αβp complexes observed in the presence of LHVS via a limited exchange between Iip10 and antigenic peptide. In fact, such functional interaction of HLA-DM with Ii processing intermediates that have not yet reached the CLIP stage has been demonstrated [55].

Selective elimination of CatS activity neither influences the subcellular distribution of class II nor the kinetics of class II surface delivery in human BLC, in contrast to the picture

observed in murine DC or leupeptin-treated BLC [18, 29, 31, 53, 54]. However, leupeptin not only blocks a plethora of cysteine and serine proteases in addition to CatS but also affects endocytic transport per se, as it reduces the transport of endocytosed material to the prelysosomal compartment [56]. Thus, the discrepancy observed between the effect of nanomolar concentrations of LHVS, which are bona fide selective for CatS [7, 33, 34, 47], and leupeptin on class II distribution and its surface deposition in human BLC is likely to be a result of the inhibitory effect of leupeptin on additional cysteine and/or serine proteases, which interact with Ii and/or other unknown factors involved in endocytic transport in BLC.

In summary, we suggest the following model: Different endocytic compartments of human BLC contain distinct patterns of protease activity with CatZ and CatB present in early and late endosomal compartments and CatS, CatD, CatH, CatC, and AEP in late endosomal and lysosomal fractions. This pattern of protease distribution largely determines the subcellular location of Ii processing, which is completed in late endosomes containing the entire spectrum of proteolytic activity tested. Conversion of Iip10 into CLIP relies on CatS activity in human BLC and is performed along the entire endocytic route, in agreement with the subcellular distribution of active CatS. CatS activity and elimination of Iip10 are not required for normal intracellular distribution and surface delivery of class II in human BLC although leupeptin blocks class II transport in this type of cell. Therefore, additional, as-yet unidentified, leupeptin-sensitive serine and/or cysteine proteases that may or may not affect Iip10 processing are likely to be involved in regulating class II transport in human BLC.

ACKNOWLEDGMENTS

The Deutsche Forschungsgemeinschaft (DR378.2-1) as well as a grant from the Federal Ministry of Education and Research (Fö.01KS9602) and the Interdisciplinary Center of Clinical Research Tübingen (IZKF) supported this work. A. L. and M. K. contributed equally to the work. We thank C. Watts for providing anti-AEP reagents.

REFERENCES

1. Wolf, P. R., Ploegh, H. L. (1995) How MHC class II molecules acquire peptide cargo: biosynthesis and trafficking through the endocytic pathway. *Annu. Rev. Cell Dev. Biol.* **11,** 267–306.
2. Villadangos, J. A., Ploegh, H. L. (2000) Proteolysis in MHC class II antigen presentation: who's in charge? *Immunity* **12,** 233–239.
3. Chapman, H. A. (1998) Endosomal proteolysis and MHC class II function. *Curr. Opin. Immunol.* **10,** 93–102.
4. Manoury, B., Hewitt, E. W., Morrice, N., Dando, P. M., Barrett, A. J., Watts, C. (1998) An asparaginyl endopeptidase processes a microbial antigen for class II MHC presentation. *Nature* **396,** 695–699.
5. Chapman, H. A., Riese, R. J., Shi, G. P. (1997) Emerging roles for cysteine proteases in human biology. *Annu. Rev. Physiol.* **59,** 63–88.
6. Beck, H., Schwarz, G., Schroter, C. J., Deeg, M., Baier, D., Stevanovic, S., Weber, E., Driessen, C., Kalbacher, H. (2001) Cathepsin S and an asparagine-specific endoprotease dominate the proteolytic processing of human myelin basic protein in vitro. *Eur. J. Immunol.* **31,** 3726–3736.
7. Riese, R. J., Wolf, P. R., Bromme, D., Natkin, L. R., Villadangos, J. A., Ploegh, H. L., Chapman, H. A. (1996) Essential role for cathepsin S in the MHC class II-associated invariant chain proecessing and peptide loading. *Immunity* **4,** 357–366.
8. Nakagawa, T., Roth, W., Wong, P., Nelson, A., Farr, A., Deussing, J., Villadangos, J. A., Ploegh, H., Peters, C., Rudensky, A. Y. (1998) Cathepsin L: critical role in li degradation and CD4 T cell selection in the thymus. *Science* **280,** 450–453.
9. Deussing, J., Roth, W., Saftig, P., Peters, C., Ploegh, H. L., Villadangos, J. A. (1998) Cathepsins B and D are dispensable for major histocompatibility complex class II-mediated antigen presentation. *Proc. Natl. Acad. Sci. USA* **95,** 4516–4521.
10. Driessen, C., Lennon-Dumenil, A. M., Ploegh, H. L. (2001) Individual cathepsins degrade immune complexes internalized by antigen-presenting cells via Fcγ receptors. *Eur. J. Immunol.* **31,** 1592–1601.
11. Pluger, E. B., Boes, M., Alfonso, C., Schroter, C. J., Kalbacher, H., Ploegh, H. L., Driessen, C. (2002) Specific role for cathepsin S in the generation of antigenic peptides in vivo. *Eur. J. Immunol.* **32,** 467–476.
12. Riese, R. J., Chapman, H. A. (2000) Cathepsins and compartmentalization in antigen presentation. *Curr. Opin. Immunol.* **12,** 107–113.
13. Lennon-Dumenil, A. M., Bakker, A. H., Maehr, R., Fiebiger, E., Overkleeft, H. S., Rosemblatt, M., Ploegh, H. L., Lagaudriere-Gesbert, C. (2002) Analysis of protease activity in live antigen-presenting cells shows regulation of the phagosomal proteolytic contents during dendritic cell activation. *J. Exp. Med.* **196,** 529–540.
14. Neefjes, J. J., Stollorz, V., Peters, P. J., Geuze, H. J., Ploegh, H. L. (1990) The biosynthetic pathway of MHC class II but not class I molecules intersects the endocytic route. *Cell* **61,** 171–183.
15. Peters, P. J., Neefjes, J. J., Oorschot, V., Ploegh, H. L., Geuze, H. J. (1991) Segregation of MHC class II molecules from MHC class I molecules in the Golgi complex for transport to lysosomal compartments. *Nature* **349,** 669–676.
16. Peters, P. J., Raposo, G., Neefjes, J. J., Oorschot, V., Leijendekker, R. L., Geuze, H. J., Ploegh, H. L. (1995) Major histocompatibility complex class II compartments in human B lymphoblastoid cells are distinct from early endosomes. *J. Exp. Med.* **182,** 325–334.
17. Kleijmeer, M. J., Morkowski, S., Griffith, J. M., Rudensky, A. Y., Geuze, H. J. (1997) Major histocompatibility complex class II compartments in human and mouse B lymphoblasts represent conventional endocytic compartments. *J. Cell Biol.* **139,** 639–649.
18. Maric, M. A., Taylor, M. D., Blum, J. S. (1994) Endosomal aspartic proteinases are required for invariant-chain processing. *Proc. Natl. Acad. Sci. USA* **91,** 2171–2175.
19. Romagnoli, P., Layet, C., Yewdell, J., Bakke, O., Germain, R. N. (1993) Relationship between invariant chain expression and major histocompatibility complex class II transport into early and late endocytic compartments. *J. Exp. Med.* **177,** 583–596.
20. Blum, J. S., Cresswell, P. (1988) Role for intracellular proteases in the processing and transport of class II HLA antigens. *Proc. Natl. Acad. Sci. USA* **85,** 3975–3979.
21. Manoury, B., Mazzeo, D., Li, D. N., Billson, J., Loak, K., Benaroch, P., Watts, C. (2003) Asparagine endopeptidase can initiate the removal of the MHC class II invariant chain chaperone. *Immunity* **18,** 489–498.
22. Roche, P. A., Cresswell, P. (1991) Proteolysis of the class II-associated invariant chain generates a peptide-binding site in intracellular HLA-DR molecules. *Proc. Natl. Acad. Sci. USA* **88,** 3150–3154.
23. Fiebiger, E., Meraner, P., Weber, E., Fang, I. F., Stingl, G., Ploegh, H., Maurer, D. (2001) Cytokines regulate proteolysis in major histocompatibility complex class II-dependent antigen presentation by dendritic cells. *J. Exp. Med.* **193,** 881–892.
24. Morton, P. A., Zacheis, M. L., Giacoletto, K. S., Manning, J. A., Schwartz, B. D. (1995) Delivery of nascent MHC class II-invariant chain complexes to lysosomal compartments, and proteolysis of invariant chain by cysteine proteases precedes peptide binding in B-lymphoblastoid cells. *J. Immunol.* **154,** 137–150.
25. Nakagawa, T. Y., Rudensky, A. Y. (1999) The role of lysosomal proteinases in MHC class II-mediated antigen processing and presentation. *Immunol. Rev.* **172,** 121–129.
26. Greiner, A., Lautwein, A., Overkleeft, H. S., Weber, E., Driessen, C. (2003) Activity and subcellular distribution of cathepsins in primary human monocytes. *J. Leukoc. Biol.* **73,** 235–242.
27. Guagliardi, L. E., Koppelman, B., Blum, J. S., Marks, M. S., Cresswell, P., Brodsky, F. M. (1990) Co-localization of molecules involved in antigen processing and presentation in an early endocytic compartment. *Nature* **343,** 133–139.
28. Drake, J. R., Lewis, T. A., Condon, K. B., Mitchell, R. N., Webster, P. (1999) Involvement of MIIC-like late endosomes in B cell receptor-mediated antigen processing in murine B cells. *J. Immunol.* **162,** 1150–1155.

29. Neefjes, J. J., Ploegh, H. L. (1992) Inhibition of endosomal proteolytic activity by leupeptin blocks surface expression of MHC class II molecules and their conversion to SDS resistance α β heterodimers in endosomes. *EMBO J.* **11,** 411–416.
30. Pieters, J., Horstmann, H., Bakke, O., Griffiths, G., Lipp, J. (1991) Intracellular transport and localization of major histocompatibility complex class II molecules and associated invariant chain. *J. Cell Biol.* **115,** 1213–1223.
31. Loss Jr., G. E., Sant, A. J. (1993) Invariant chain retains MHC class II molecules in the endocytic pathway. *J. Immunol.* **150,** 3187–3197.
32. Shi, G. P., Villadangos, J. A., Dranoff, G., Small, C., Gu, L., Haley, K. J., Riese, R., Ploegh, H. L., Chapman, H. A. (1999) Cathepsin S required for normal MHC class II peptide loading and germinal center development. *Immunity* **10,** 197–206.
33. Wiendl, H., Lautwein, A., Mitsdorffer, M., Krause, S., Erfurth, S., Wienhold, W., Morgalla, M., Weber, E., Overkleeft, H. S., Lochmuller, H., Melms, A., Tolosa, E., Driessen, C. (2003) Antigen processing and presentation in human muscle: cathepsin S is critical for MHC class II expression and upregulated in inflammatory myopathies. *J. Neuroimmunol.* **138,** 132–143.
34. Driessen, C., Bryant, R. A., Lennon-Dumenil, A. M., Villadangos, J. A., Bryant, P. W., Shi, G. P., Chapman, H. A., Ploegh, H. L. (1999) Cathepsin S controls the trafficking and maturation of MHC class II molecules in dendritic cells. *J. Cell Biol.* **147,** 775–790.
35. Pierre, P., Turley, S. J., Gatti, E., Hull, M., Meltzer, J., Mirza, A., Inaba, K., Steinman, R. M., Mellman, I. (1997) Developmental regulation of MHC class II transport in mouse dendritic cells. *Nature* **388,** 787–792.
36. Lautwein, A., Burster, T., Lennon-Dumenil, A. M., Overkleeft, H. S., Weber, E., Kalbacher, H., Driessen, C. (2002) Inflammatory stimuli recruit cathepsin activity to late endosomal compartments in human dendritic cells. *Eur. J. Immunol.* **32,** 3348–3357.
37. Kleijmeer, M., Ramm, G., Schuurhuis, D., Griffith, J., Rescigno, M., Ricciardi-Castagnoli, P., Rudensky, A. Y., Ossendorp, F., Melief, C. J., Stoorvogel, W., Geuze, H. J. (2001) Reorganization of multivesicular bodies regulates MHC class II antigen presentation by dendritic cells. *J. Cell Biol.* **155,** 53–63.
38. Greenbaum, D., Medzihradszky, K. F., Burlingame, A., Bogyo, M. (2000) Epoxide electrophiles as activity-dependent cysteine protease profiling and discovery tools. *Chem. Biol.* **7,** 569–581.
39. Shi, G. P., Bryant, R. A., Riese, R., Verhelst, S., Driessen, C., Li, Z., Bromme, D., Ploegh, H. L., Chapman, H. A. (2000) Role for cathepsin F in invariant chain processing and major histocompatibility complex class II peptide loading by macrophages. *J. Exp. Med.* **191,** 1177–1186.
40. Palmer, J. T., Rasnick, D., Klaus, J. L., Bromme, D. (1995) Vinyl sulfones as mechanism-based cysteine protease inhibitors. *J. Med. Chem.* **38,** 3193–3196.
41. Villadangos, J. A., Driessen, C., Shi, G. P., Chapman, H. A., Ploegh, H. L. (2000) Early endosomal maturation of MHC class II molecules independently of cysteine proteases and H-2DM. *EMBO J.* **19,** 882–891.
42. Schroter, C. J., Braun, M., Englert, J., Beck, H., Schmid, H., Kalbacher, H. (1999) A rapid method to separate endosomes from lysosomal contents using differential centrifugation and hypotonic lysis of lysosomes. *J. Immunol. Methods* **227,** 161–168.
43. Castellino, F., Germain, R. N. (1995) Extensive trafficking of MHC class II-invariant chain complexes in the endocytic pathway and appearance of peptide-loaded class II in multiple compartments. *Immunity* **2,** 73–88.
44. Shevchenko, A., Wilm, M., Vorm, O., Mann, M. (1996) Mass spectrometric sequencing of proteins silver-stained polyacrylamide gels. *Anal. Chem.* **68,** 850–858.
45. Perkins, D. N., Pappin, D. J., Creasy, D. M., Cottrell, J. S. (1999) Probability-based protein identification by searching sequence databases using mass spectrometry data. *Electrophoresis* **20,** 3551–3567.
46. Villadangos, J. A., Bryant, R. A., Deussing, J., Driessen, C., Lennon-Dumenil, A. M., Riese, R. J., Roth, W., Saftig, P., Shi, G. P., Chapman, H. A., Peters, C., Ploegh, H. L. (1999) Proteases involved in MHC class II antigen presentation. *Immunol. Rev.* **172,** 109–120.
47. Villadangos, J. A., Riese, R. J., Peters, C., Chapman, H. A., Ploegh, H. L. (1997) Degradation of mouse invariant chain: roles of cathepsins S and D and the influence of major histocompatibility complex polymorphism. *J. Exp. Med.* **186,** 549–560.
48. Benaroch, P., Yilla, M., Raposo, G., Ito, K., Miwa, K., Geuze, H. J., Ploegh, H. L. (1995) How MHC class II molecules reach the endocytic pathway. *EMBO J.* **14,** 37–49.
49. Kleijmeer, M. J., Ossevoort, M. A., van Veen, C. J., van Hellemond, J. J., Neefjes, J. J., Kast, W. M., Melief, C. J., Geuze, H. J. (1995) MHC class II compartments and the kinetics of antigen presentation in activated mouse spleen dendritic cells. *J. Immunol.* **154,** 5715–5724.
50. Garin, J., Diez, R., Kieffer, S., Dermine, J. F., Duclos, S., Gagnon, E., Sadoul, R., Rondeau, C., Desjardins, M. (2001) The phagosome proteome: insight into phagosome functions. *J. Cell Biol.* **152,** 165–180.
51. Pierre, P., Mellman, I. (1998) Developmental regulation of invariant chain proteolysis controls MHC class II trafficking in mouse dendritic cells. *Cell* **93,** 1135–1145.
52. Villadangos, J. A., Cardoso, M., Steptoe, R. J., van Berkel, D., Pooley, J., Carbone, F. R., Shortman, K. (2001) MHC class II expression is regulated in dendritic cells independently of invariant chain degradation. *Immunity* **14,** 739–749.
53. Amigorena, S., Webster, P., Drake, J., Newcomb, J., Cresswell, P., Mellman, I. (1995) Invariant chain cleavage and peptide loading in major histocompatibility complex class II vesicles. *J. Exp. Med.* **181,** 1729–1741.
54. Brachet, V., Raposo, G., Amigorena, S., Mellman, I. (1997) Ii chain controls the transport of major histocompatibility complex class II molecules to and from lysosomes. *J. Cell Biol.* **137,** 51–65.
55. Denzin, L. K., Hammond, C., Cresswell, P. (1996) HLA-DM interactions with intermediates in HLA-DR maturation and a role for HLA-DM in stabilizing empty HLA-DR molecules. *J. Exp. Med.* **184,** 2153–2165.
56. Zachgo, S., Dobberstein, B., Griffiths, G. (1992) A block in degradation of MHC class II-associated invariant chain correlates with a reduction in transport from endosome carrier vesicles to the prelysosome compartment. *J. Cell Sci.* **103,** 811–822.